Polarimetry: From the Sun to Stars and Stellar Environments
Proceedings IAU Symposium No. 305, 2014
K. N. Nagendra, S. Bagnulo, R. Centeno &
M. J. Martínez González, eds.

doi:10.1017/S1743921315004585

Magnetic field configuration in a flaring active region

J. Palacios[1], L. A. Balmaceda[2,3] and L. E. Vieira[2]

[1]Space Reseach Group–Space Weather, Departamento de Física y Matemáticas,
Universidad de Alcalá
University Campus, Sciences Building, P.O. 28871, Alcalá de Henares, Spain
email: judith.palacios@uah.es
[2]Instituto Nacional de Pesquisas Espaciais (INPE),
Avda. dos Astronautas, São José dos Campos–SP, 12227-010, Brazil
[3]Instituto de Ciencias Astronómicas, de la Tierra y el Espacio, ICATE-CONICET
Avda. de España Sur 1512, J5402DSP, San Juan, Argentina

Abstract. The Helioseismic and Magnetic Imager (HMI) on board the Solar Dynamics Observatory (SDO) provides continuous monitoring of the Sun's vector magnetic field through full-disk photospheric data with both high cadence and high spatial resolution. Here we investigate the evolution of AR 11249 from March 6 to March 7, 2012. We make use of HMI Stokes imaging, SDO/SHARPs, the HMI magnetic field line-of-sight (LOS) maps and the transverse components of the magnetic field as well as LOS velocity maps in order to detect regions with significant flux emergence and/or cancellation. In addition, we apply the Local Correlation Tracking (LCT) technique to the total and signed magnetic flux data and derive maps of horizontal velocity. From this analysis, we were able to pinpoint localized shear regions (and a shear channel) where penumbrae and pore formation areas, with strong linear polarization signals, are stretched and squeezed, showing also important downflows and upflows. We have also utilized Hinode/SP data and compared them to the HMI-SHARPs and the HMI-Stokes spectrograms. The aforementioned shear channel seems to correspond well with the X-class flare main channel of March 7 2012, as observed in AIA/SDO 171, 304 and 1600 Å.

Keywords. Sun: photosphere, magnetic fields, flares; techniques: polarimetric

1. Introduction

Solar flares are one of the most extreme phenomena in the atmosphere of the Sun, releasing enormous quantities of energy in very short timescales (e.g., Benz 2008). High resolution magnetic field data represent an invaluable tool to investigate the conditions and changes in the regions where such phenomena take place.

Here, we study the temporal and spatial evolution of active region AR 11429 (N17E15) associated to an intense flaring activity observed during 2012 March 6 to 9. In particular, we study the evolution of the photospheric magnetic field in this active region, and the variations from its original configuration. For this purpose, we use a time series of vector field maps with high spatial and temporal resolution obtained with the Hinode/SP and the SDO/HMI instruments.

2. Data

The Helioseismic and Magnetic Imager (HMI, Scherrer *et al.* 2008) on board the Solar Dynamics Observatory (SDO, Pesnell *et al.* 2012) provides continuous monitoring of the Sun's vector magnetic field through full-disk photospheric data with both high cadence and high spatial resolution.

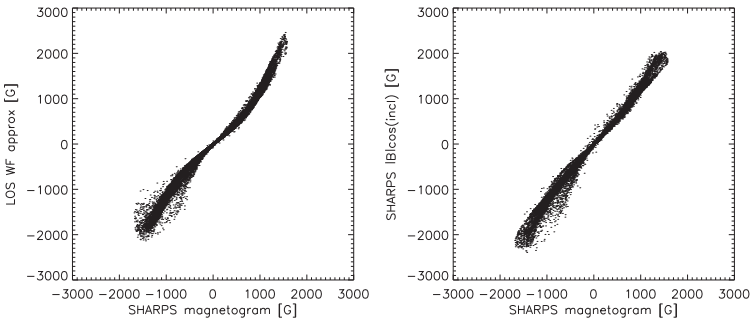

Figure 1. *Left:* comparison between the SHARP LOS-magnetogram and the LOS-weak field approximation. *Right:* Comparison between the SHARP LOS-magnetogram and the SHARP inverted quantities.

We also made use of Hinode/SP data (Tsuneta *et al.* 2008, Ichimoto *et al.* 2008) onboard Hinode (Kosugi *et al.* 2007) to actually compare the active region at the same time.

To complete this work, we used 12-min cadence data from SDO/AIA (Lemen *et al.* 2012) in different wavelengths. GOES X-ray data (Hill *et al.* 2005) were employed as well.

2.1. *SDO/HMI*

For this work we used a whole 2-day sequence, 12-min cadence of SDO/HMI SHARPs (Space-weather HMI Active Region Patches, Bobra *et al.* 2011, Hoeksema *et al.* 2014); more specifically, we made use of the magnetic field strength, its inclination and its azimuth, and the LOS velocity (*vlos_mag*). These data were obtained from the spectral line inversion code, VFISV (Very Fast Inversion of the Stokes Vector, Borrero *et al.* 2011, Centeno *et al.* 2014). We employed SHARP line-of-sight (LOS) magnetograms as well.

In addition, we have utilized HMI full-disk Stokes spectrograms (*HMI.S_720s* data series). Extracting the Stokes profiles from the spectrograms, we computed the magnetic flux density using the weak field approximation (hereafter WF; Landi Degl'Innocenti & Landolfi 2004), considering the HMI Fe I nominal wavelength 6173.34 Å and the 69 mÅ of spectral sampling, coarsely normalizing the profiles using the red-most wavelength point of Stokes *I*.

In Fig. 1 we compare the results of the weak field approximation to the LOS magnetograms. Being aware that the measured magnetic fields are in the strong field regime (but still in the usual solar range), we compared the WF maps to the SHARP LOS-magnetograms. These different estimates turn out to agree rather well quantitatively and show the same magnitude range for the field (around 2000 G in absolute value), as shown in the scatterplot of the left panel of Fig. 1. We also performed the comparison of the LOS-magnetograms with the HMI-SHARP quantity $B \cdot cos\gamma$, where B is the field strength and γ is its inclination. The corresponding scatterplot is displayed in the right panel of Fig. 1.

SHARP Dopplergrams (LOS velocity) and *vlos_mag* velocity maps (LOS velocity of the magnetized plasma, Hoeksema *et al.* 2014) present shifts due to the orbital motion of the satellite. For comparison, we also computed the velocities by measuring the Doppler shift of Stokes *I* for quiet Sun pixels (<250 G), obtaining very similar values to those of the SHARP Dopplergrams, with the same bulk shift due to the orbital motion of SDO (as in Hoeksema *et al.* 2014). HMI corrected velocity values are in the range between

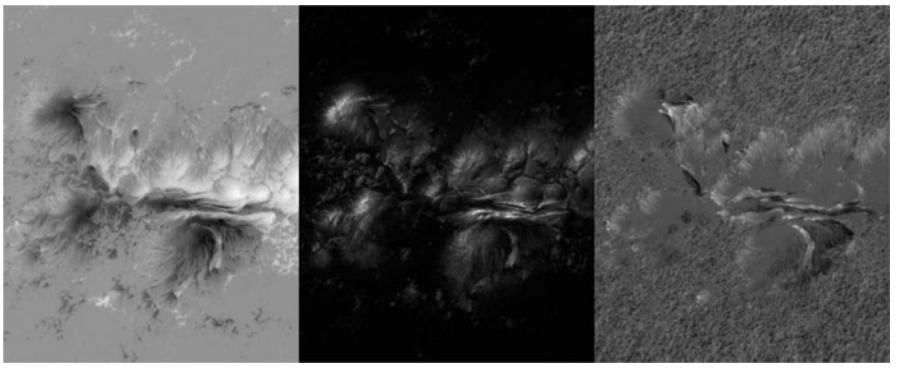

Figure 2. *From left to right*: HINODE/SOT-SP WF LOS-magnetic field (max 3500 G in absolute value); transverse field (maximum 1400 G) and Doppler velocities (ranging from –3.5 to 8.5 km s^{-1})

$\pm$ 3 km s^{-1}. To overcome this velocity offset issue, we have used Hinode SOT-SP for a further comparison.

2.2. *Hinode/SP*

Besides their high spatial sampling, $0''32$ px^{-1}, Hinode/SP data have a spectral sampling of 21.5 mÅ per pixel with a spectral window that comprises the Fe I 6301 and 6302 Å lines. Since the temporal cadence of Hinode/SP is lower than that of HMI, we show data to the closest possible time to the flare onset, i.e. at 22:10 UT. We used the Hinode/SP Stokes profiles of the Fe I 6301 Å line in order to compare them to the HMI Stokes and the HMI SHARP data (Fe I line 6173 Å). We also estimated the flux density for the longitudinal and the transverse magnetic fields, and the Doppler velocity with the same methods applied to the HMI Full Stokes spectrograms, shown in Fig. 2.

Doppler velocities from Stokes *I* reach almost 9 km s^{-1} at the east-northernmost sunspot boundary in Fig. 2 (right panel). These high speed flows are also evident in the 6301 Å continuum of Stokes *V*. However, these flows are less intense and harder to notice in the HMI Dopplergrams and the *vlos_mag* quantity of the SHARPs data.

3. Evolution of the active region

This very complex active region produced flares from C to X-type with associated coronal mass ejections that produced geomagnetic activity. The active region, consisting originally of five main sunspots, evolved from its initial configuration into an elongated region, observed in continuum and longitudinal magnetograms.

The sunspots in the middle and the trailing parts decayed while the leading spots rearranged and merged again. Regions with alternating polarities appeared and disappeared throughout the whole process. The main changes in the magnetic field were observed close to the polarity inversion line (Fig. 2, left). Flux emerged several hours prior to the occurrence of the flare, forming penumbral structures in between the large spots.

Several flares were detected on March 6 but the activity decreased after the X-class flare that took place on March 7. The aforementioned X-class flare is displayed in Fig. 3. This figure shows the X-ray flux from GOES in two energy ranges, 1-8 Å and 0.5-4 Å (top panel) and the normalized intensity in the AIA 171 Å 12-min filtergram sequence (bottom panel).

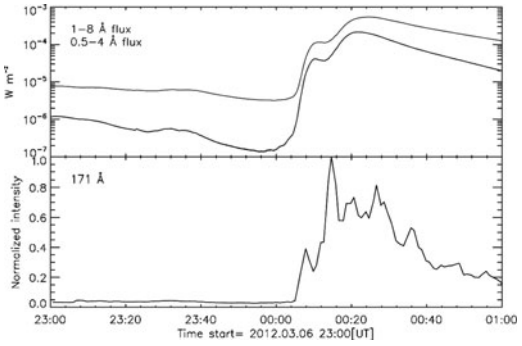

Figure 3. *Top*: X-class flare in GOES flux in 1-8 Å and 0.5-4 Å. *Bottom:* Normalized intensity of AIA 171 Å filtergrams.

Variations in the orientation and inclination of the vector magnetic field related to the largest flare onset, an X-class flare on 2012 March 7, were detected, as well as the occurrence of flux emergence and magnetic flux cancellation in the region. The center-northernmost penumbra shows significant transverse fields which are co-located with the strong line-of-sight flows.

4. Local Correlation Tracking (LCT) on HMI data

Local Correlation Tracking is a feature tracking method developed by November & Simon (1988) and implemented by Yi & Molowny-Horas (1995). This technique computes the displacement between consecutive images. A window function is applied, and the relative displacements that maximize the correlation in this window are obtained. It has a dependence on the window size and its temporal averaging. These Gaussian boxcar windows are chosen accordingly depending on the size of the structure to be tracked and time span of the event. In this case, the time span is one hour and the FWHM is $7''.5$. We have applied this method on aligned LOS-magnetograms and total magnetic field maps from the HMI-SHARP data series. Feature emergence and displacement is clearly tracked with LCT. LCT velocities and divergence patterns are equivalent for the magnetograms and the total magnetic field maps, with ~ 0.1 km s^{-1} of average horizontal tracked velocity.

5. Discussion and future work

We have observed magnetic flux emergence and cancellation associated to the flaring activity observed in AR 11429. From the vector magnetic field data, we have also observed an important shear line close to the polarity inversion lines that is spatially coincident with the flare channel. In this sheared area, strong transverse fields and line-of-sight velocities of up to ± 4 km s^{-1} were identified. Some supersonic flows that were seen in the Hinode data were not registered by the HMI instrument due to the lower spectral sampling of the latter.

Horizontal velocity maps obtained using the LCT technique revealed feature emergence and strong proper motions.

Acknowledgements

We are very grateful to the SDO HMI, AIA, Hinode/SOT and GOES teams for all valuable data. J. P. acknowledges funding from IAU to attend IAUS305 and UAH-travel

grants. She also acknowledges projects AYA2013-47735-P and the JPI mobility grants program of Banco Santander. L. B. acknowledges FAPESP 2013/03085-7.

References

Benz, A. O.,2008, *Living Rev. Solar Phys.* 5, 1

Bobra, M. G. , Sun, X., Hoeksema, J. T., Turmon, M., Liu, Y., Hayashi, K., Barnes, G., & Leka, K. D., 2014, *Solar Phys.* 289, 3549

Borrero, J. M., Tomczyk, S., Kubo, M., Socas-Navarro, H., Schou, J., Couvidat, S., & Bogart, R., 2011, *Solar Phys.* 273, 267

Centeno, R., Schou, J., Hayashi, K., Norton, A., Hoeksema, J. T., Liu, Y., Leka, K. D., & Barnes, G., 2014, *Solar Phys.* 289, 3531

Hill, S. M., Pizzo, V. J., Balch, C. C., Biesecker, D. A., Bornmann, P., Hildner, E., Lewis, L. D., Grubb, R. N., Husler, M. P., Prendergast, K., and 26 coauthors , 2005, *Solar Phys.* 226, 255

Hoeksema, J. T., Liu, Y., Hayashi, K., Sun, X., Schou, ., Couvidat, S., Norton, A., Bobra, M., Centeno, R., Leka, K. D., and 2 coauthors, 2014, *Solar Phys.* 289, 3483

Ichimoto, K., Lites, B., Elmore, D., Suematsu, Y., Tsuneta, S., Katsukawa, Y., Shimizu, T., Shine, R., Tarbell, T., Title, A., and 10 coauthors, 2008, *Solar Phys.* 249, 233

Kosugi, T., Matsuzaki, K., Sakao, T., Shimizu, T., Sone, Y., Tachikawa, S., Hashimoto, T., Minesugi, K., Ohnishi, A., Yamada, T., and 15 coauthors, 2007, *Solar Phys.* 243, 3

Landi Degl'Innocenti, L., & Landolfi, M., 2004, *ASSL* vol. 307, Kluwer Academic Publishers

Lemen, J. R., Title, A. M., Akin, D. J., Boerner, P. F., Chou, C., Drake, J. F., Duncan, D. W., Edwards, C. G., Friedlaender, F. M., Heyman, G. F., and 37 coauthors 2012, *Solar Phys.* 275, 17

November, L. J., & Simon, G. W., 1988, *ApJ* 333, 427

Pesnell, W. D., Thompson, B. J., & Chamberlin, P. C., 2012, *Solar Phys.* 275, 3

Scherrer, P. H., Schou, J., Bush, R. I., Kosovichev, A. G., Bogart, R. S., Hoeksema, J. T., Liu, Y., Duvall, T. L., Zhao, J., Title, A. M., and 3 coauthors, 2012, *Solar Phys.* 275, 207

Tsuneta, S., Ichimoto, K., Katsukawa, Y., Nagata, S., Otsubo, M., Shimizu, T., Suematsu, Y., Nakagiri, M., Noguchi, M., Tarbell, T., and 15 coauthors, 2008, *Solar Phys.* 249, 167

Yi, Z. & Molowny-Horas R., 1995, *A&A* 295, 199